Journal of Membrane Science and Research 6 (2020) 351-358

Journal of Membrane Science & Research

journal homepage: www.msrjournal.com

Research Paper

Effect of Surface Modification with Electrospun Nanofibers on the Performance of an Ultrafiltration Membrane

Ladan Zoka [1], Roberto M. Narbaitz [1], Takeshi Matsuura [2,*]

[1] *Department of Civil Engineering, University of Ottawa, 161 Louis Pasteur, Ottawa, K1N 6N5, ON, Canada*
[2] *Department of Chemical and Biological Engineering, University of Ottawa, 161 Louis Pasteur, Ottawa, K1N 6N5, ON, Canada*

Article info

Received 2020-01-02
Revised 2020-04-26
Accepted 2020-04-27
Available online 2020-04-27

Keywords

Ultrafiltration membrane
Surface coating
PVDF nanofibers
Pure water permeation flux
River water fouling
Protein fouling

Highlights

- A commercial PES membrane was coated with electrospun PVDF nanofiber layers.
- The composite membrane had higher pure water fluxes than the base PES membrane.
- The composite membrane fouled more readily due to foulant entrapment.
- Increased electrospinning time increased the surface hydrophobicity.
- The new membrane's nanofiber mat did not impact the separation of protein solutes.

Graphical abstract

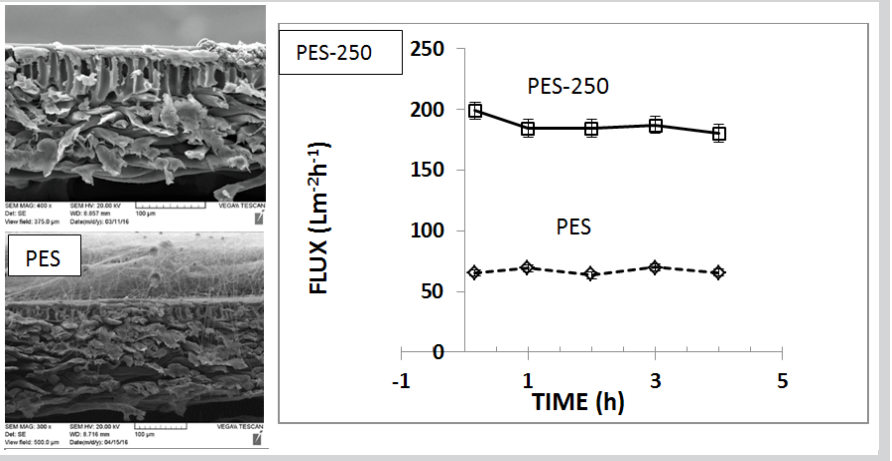

Abstract

Electrospinning of nanofibrous mats to create new membranes has been widely investigated, however surface modification of commercial membranes by electrospinning of nanofiber layer has received limited attention. In this work, the surface of a commercial polyethersulfone (PES) ultrafiltration membrane was coated with electrospun polyvinylidene fluoride (PVDF) hydrophobic nanofibers (NFs) for different time periods, i.e., 25 min, 125 min, and 250 min., and the effect of coating on the filtration performance was investigated. The membranes were characterized by scanning electron microscopy (SEM), contact angle measurement and further subjected to pure water permeation experiments, as well as the filtration of Ottawa River Water (ORW) and various protein solutes. By a thorough statistical analysis, it was concluded that the coating with the electrospun nanofiber layer enhanced the pure water permeation (PWP) flux. However, the fouling of the composite nanofiber/PES membranes was more severe due to the compaction of the soft nanofiber layer and the entrapment of foulants in the spaces between nanofibers. The nanofiber mat did not impact the separation of protein solutes as the composite and base PES membranes had the same protein removals.

1. Introduction

The technique to fabricate nanofibrous mats by electro-spinning has been known for many years. But the application of the electrospun nanofiber mats, also known as electro-spun nanofiber membranes (ENMs), has been limited to particles removal from air, a process that has already been commercialized (e.g. Donaldson (USA)) [1]. Despite its short history, in contrast to air cleaning, some companies have emerged recently for the application of ENMs for liquid separation (e.g. Pardem (Czech Republic), SPUR Nanotechnologies (Czech Republic), Liquidity Corporation (USA)) [2]. Moreover, a large number of researches on this subject are reported in the open literature every year, e.g. [3-6]. As well, many papers are now available for the pressure driven membrane separation processes such as nanofiltration (NF) [7], ultrafiltration (UF) [8], microfiltration (MF) [9,10] by ENMs, and an equally large number of papers have been published for the other membrane separation processes such as pervaporation (PV) [11], membrane distillation (MD) [12], forward osmosis (FO) [13] and membrane adsorption (MA) [14]. The reason that ENMs have become one of the most popular research topics is their unique features such as facile fabrication, interconnectivity and large volume/area ratio. Among various methods for the fabrication of ENMs based

* Corresponding author: matsuura@uottawa.ca (T. Matsuura)

DOI: 10.22079/JMSR.2020.119481.1319

membranes, multilayered composite membranes (with one or two ENMs layers) are the most commonly used for the filtration of aqueous solutions [15]. However, surface modification of commercial membranes by electrospinning of nanofiber layer has rarely been done.

Recently, Dobosz et al. [16] fabricated multilayered composite membranes by electrospinning cellulose or polysulfone layers on top of commercial ultrafiltration membranes and found that the pure water permeation flux was increased when polysulfone ENM layer was coated on the substrate UF membrane while preserving the selectivity of the UF membrane almost intact. Interestingly, the flux enhancement occurred when the coating layer consisted of relatively hydrophobic PES nanofibers, but did not occur when coating layer consisted of the more hydrophilic cellulose nanofibers [16]. They have speculated that the enhanced pure water fluxes in their experiments were due to the randomly oriented nanofibers with zigzag configurations (with different distances from the substrate membrane surface). This was based on the beneficial impact of zig-zag spacers identified by Ma and Song [17] and Won et al. [18] in their simulations modeling concentration polarization. Since Dobosz et al. [16] pertain to pure water fluxes in which there is no concentration polarization their hypothesized mechanism for the enhanced flux seems questionable.

Furthermore, Wang et al. reported the directional water transport induced by asymmetric wettability across fabrics [19]. They have prepared polyester fabric with two surfaces, one hydrophobic and the other hydrophilic. When the pressure necessary to allow water to break through the fabric was measured, 1.77 kPa was required to transfer water from the hydrophilic to the hydrophobic side, whereas only 0.19 kPa was required for water transfer in the opposite direction. They ascribed this phenomenon to the draw of water from the hydrophobic to the hydrophilic pores or the evaporation of water on the hydrophobic pore surface and condensation in the hydrophilic pore. But the exact mechanism of water transport through the fabric of wettability gradient is still unknown.

A composite membrane comprised of a hydrophobic nanofiber layer coated on top of a hydrophilic substrate layer seems a typical example of the membranes with wettability gradient. Commercial PES membranes deform with time as evident from long term tests, such as those performed by Dang et al. [20]. It can also be hypothesized that a modified PES membrane created by placing an electrospun layer on a commercial PES membrane will be stronger so that its pores deform less than those of the commercial PES membrane and/or the larger pores of the hydrophobic electrospun layer will channel the flow, resulting in less friction and higher fluxes in electrospun membranes [21].

This work reports on a study on the performance of ENM membranes prepared by coating a polyethersulfone commercial membrane with electrospun nanofibers of a more hydrophobic polymer. The manuscript presents the results of the lead author's thesis [21] which was initiated well before the publication of Dobosz et al. [16]. Given the findings of Dobosz et al. [16] the objectives of this manuscript are to confirm the pure water permeation flux enhancement after the coating of hydrophobic ENMs on a commercial ultrafiltration membrane and to further investigate the fouling of this type of membrane using Ottawa River (OR) water and various protein solutions. PVDF was chosen for the material of ENMs since PVDF is known to be more hydrophobic than PES.

2. Materials and Methods

2.1. Materials

The polyethersulfone (PES) membrane with a nominal molecular cut off (MWCO) of 30 kD was procured from Synder Filtration (Vacaville, CA). Polyvinylidene fluoride (PVDF, Kynar 740, Arkema Inc., Philadelphia, PA) was used to prepare electrospun nanofibers. Acetone and dimethylacetamide (DMAC) were purchased from Sigma-Aldrich (St. Louis, MO).

Trypsin (MW=23.8 kDa), pepsin (MW=35 kDa), egg albumin (MW=45 kDa with a purity of 62-88 %) and bovine serum albumin (BSA, MW = 66 kDa and a purity of 96%) were also purchased from Sigma-Aldrich (St. Louis, MO). Raw Ottawa River water (ORW) sample was collected from the intake of the Britannia Water Treatment Plant in Ottawa, Ontario during the winter of 2015. This river has few particles (i.e., low turbidity), low inorganic content (i.e., low hardness and alkalinity) and significant natural organic matter (NOM), thus the principal foulant in this water is expected to be the NOM [22,23].

2.2. Membrane electrospinning

The surface of the PES membrane was coated with PVDF nanofibers following the method described by Efome et al. [24]. The spinning dope (15 wt% PVDF, 34 wt% DMAC, and 51 wt% acetone) was prepared by adding the polymer to the solvent and by vigorously stirring (180 rpm) of the mixture for 24 h in an orbital shaker at 50°C. After cooling, the spinning dope was transferred to the syringe within the electrospinning equipment which was supplied by Beijing Ucalery Technology and Development Co., LTD, China. Within this apparatus, a sheet of the commercial PES membrane was wrapped around a drum that rotated at 140 rpm, and the tip of the dope syringe was located at 150 mm from the drum. Electrodes were connected to the drum and the tip of the syringe to create a circuit, and the applied voltage of 15 kV caused a nanofiber of the dope to be drawn from the syringe tip to the drum. Electrospinning was conducted for three different periods: 25, 125, and 250 minutes. The commercial PES UF membrane is coded as PES. Electrospun membranes are coded as EPES-x, where x is the electrospinning period (min).

2.3. Membrane characterization

The commercial PES membrane and the nanofiber coated membranes were characterized by scanning electron microscopy (SEM) and contact angle measurements.

2.3.1. Scanning electron microscope (SEM)

A scanning electron microscope, model Vegall XMU (Tescan, Warrendale, PA, USA) was used to investigate the surface and cross-sectional morphology of the membranes before and after filtration experiments with ORW (The membranes were dried for two days after the ORW filtration.). For the cross-sectional images, the membrane was soaked in liquid nitrogen and the frozen membrane was cut into pieces with sharp scissors. In order to increase electron conductivity, the samples were gold-sputtered to a thickness of 10 nm in a coater (Quorum Q 150T, Britain).

2.3.2. Contact angle measurements

A computer-controlled digital camera based system (VCA Optima Surface Analysis system, AST Products Inc., Billerica, MA) was used to measure the advancing contact angle. The membranes were cut into small pieces (10×15 mm) and placed on micro slides (25×75×1 mm) prior to being placed in the analyzer. The volume of the water droplet used for each measurement was 1.5 µL [25]. For each sample, the contact angle was measured twice on each of 20 locations and the average was reported.

2.3.3. Membrane filtration tests

The filtration test was conducted with three conventional cross-flow cells, each with an effective membrane area of 2.04 x 10^{-3} m^2, connected in series. For a detailed description of the membrane cells and the filtration system refer to Mosqueda-Jimenez et al. [26] and Zoka [21]. The feed flow was maintained at 1.1 L/min to minimize the concentration polarization effect.

The membrane filtration testing procedure consisted of the following phases: pre-compaction under pure water at 70 psig, pure water permeation test at 50 psig, fouling test (filtration of either ORW or protein solutions) at 50 psig, and tangential flow cleaning test. Each phase lasted 4 h. Each membrane type was tested in triplicate (one coupon in each of the three cross-flow cells), the values presented in the results sections are the average of the three sets of results.

During the pure water permeation, the permeate volume, V (L), collected during the period t (h) was measured and the pure water permeation flux, PWP (Lm^{-2} h^{-1}) was calculated by

$$PWP = V/(At) \quad (1)$$

where A is the effective membrane area (2.04 x 10^{-3} m^2).

In the filtration test with the feed ORW or protein solutions, the permeate samples were collected every hour to determine the permeate flux. The permeate flux, J ($Lm^{-2}h^{-1}$), was calculated by equation (1) using J instead of PWP. In case of the filtration of the protein solution, the concentration of protein in the permeate samples was measured using a UV spectrophotometer (DR 6000, Hach Instruments, Loveland, CO). The solute separation, R, was then calculated by:

$$R = 1-(C_p/C_f) \quad (2)$$

where C_p and C_f are permeate and feed protein concentrations, respectively. The concentrations of the various protein solutions tested were approximately 100 mg L^{-1}.

In the tangential cleaning test, the membrane was cleaned by the

tangential flow of distilled water. During the period of 4 h, the permeate flux was determined every hour.

2.3.4. Statistical analysis

The PWP fluxes of the EPES and control PES membranes were compared using the t-tests assuming a constant variance, they were performed with the help of Microsoft Excel®. The ± cited with the data presented refers to one standard deviation.

3. Results and discussion

3.1. Pure water permeation

Table 1 shows the results of the PWP experiments. An explanation of the grouping of experimental results in series is in order. There is a considerable variation in the PES membrane flux from membrane sheet to membrane sheet and from coupon to coupon, taken from the same sheet, even though the membrane was purchased from a membrane manufacturer. Usually, the variation from coupon to coupon (from the same sheet) is less than the variation from sheet to sheet. Therefore, in each series of the experiments shown in Table 1, the membrane coupons were taken from the same sheet and electro-spinning was applied on those coupons to investigate the effect of electro-spinning. Thus, the flux variation between different membrane sheets could be eliminated from the effect of electrospinning on the *PWP*. For instance, in the series 1 experiments, the control PES membrane coupons and the coupons on which 250 min of electro-spinning was applied (EPES-250) were from the same sheet.

Table 1
Results of PWP experiments [a]

Series	Membrane	Average PWP ($Lm^{-2}h^{-1}$)
1	PES	66.6
	EPES-250	189.6
2	PES	98.6
3	PES	123.6
	EPES-25	141.1
	EPES-125	140.0
	EPES-250	156.1
4	PES	127.0
	EPES-25	173.9
	EPES-125	113.6
	EPES-250	241.8

[a] By using series 1 membranes, the lead author found the *PWP* increase. Those membranes were further used for ORW filtration experiments. Series 3 and 4 membranes were used to know the effect of electrospinning period more thoroughly. These spinning periods were chosen to make the nanofiber thickness comparable to but lower than the thickness of the pristine UF membrane. As well, the lowest thickness was chosen so that it was enough to detect the effect of coating on PWP.

In each series of Table 1, *PWP*s from the EPES membranes are larger than that of the control PES membrane with only one exception of Series 4 EPES-125 which was confirmed by repeated experiments. It may therefore reasonably be concluded that the electro-spinning of PVDF nanofiber layer on the control PES increased the *PWP*. To confirm the conclusion, the statistical t–test was performed. For this purpose, the data in Table 1 were grouped into variable 1, which includes all the PES data, and variable 2, which includes all the EPES data. A t-test was performed assuming equal variances with the null hypothesis that these two groups of data (variables 1 and 2) are from the same sample body. The justification for the assumption of equal variances is that all data were collected with the same PWP experimental protocol. Microsoft Excel® was used to facilitate the statistical data analysis. With a degree of freedom of 9 (= 11 data points – 2 groups), the t statistic was calculated as -2.59464, which was less than the negative t critical for one-tail (-1.833113) and two-tails (-2.262157). Therefore, the null hypothesis was rejected with 95% confidence based on both one- and two-tails. This confirms that the PWP data for EPES membrane came from a different sample body (with larger flux value) than those of PES.

Figure 1 shows the change of *PWP* with time for the PES and EPES-250 membranes in Series 1. While the PWP of the PES membrane remained constant during the 4 h test, EPES-250 membrane exhibited a slight flux decline, suggesting that the PVDF electro-spun layer on the EPES-250 membrane was more severely compacted than the support PES membrane.

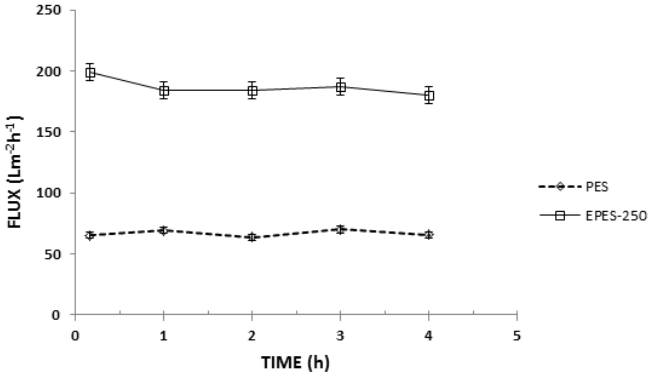

Fig. 1. Change of *PWP* during the PWP experiments with time for series 1 membranes.

3.2. Filtration of Ottawa River Water (ORW)

The PWP test (using distilled water as feed) with the series 1 membranes was followed by the filtration test with ORW as feed, these tests were performed with coupons of the EPES-250 and control PES membranes. Figure 2 shows that the initial permeate flux of EPES-250 membrane for ORW (140 $Lm^{-2}h^{-1}$) was much lower than the *PWP* (average PWP = 189.62 $Lm^{-2}h^{-1}$ as seen in Figure 1) and it kept decreasing with time. In contrast, the permeate flux of PES was only slightly lower than the *PWP* (66.6 $Lm^{-2}h^{-1}$) and it was stable. Nevertheless, the permeate flux of EPES-250 was significantly higher than PES during the 4 h filtration period.

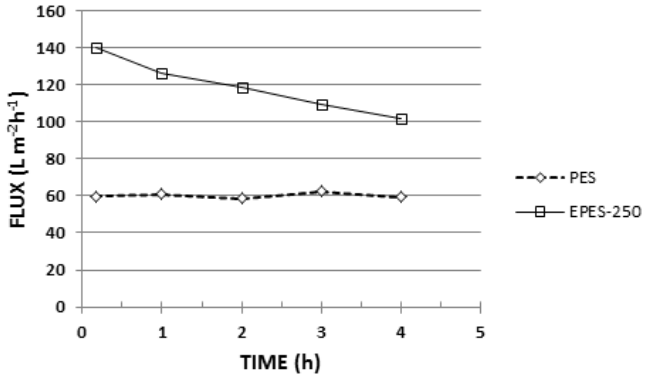

Fig. 2. The permeate flux data of ORW.

The ORW fouling data shown in Figures 1 and 2, together with the post-fouling *PWP* data (i.e., the distilled water tangential cleaning step), were further analyzed by flux decrease due to compaction, *Comp*, total, R_{total}, irreversible, R_{irr}, and irreversible, R_{rev}, fouling [27]. Those parameters are defined by,

$$Compac = (Jw_0 - Jw_1) / (J_{w0}) \quad (3)$$

$$R_{total} = (Jw_1 - Jp) / Jw_1 \quad (4)$$

$$R_{irr} = (Jw_1 - Jw_2) / Jw_1 \quad (5)$$

$$R_{rev} = (Jw_2 - Jp) / Jw_1 \quad (6)$$

where Jw_0 is the first pure water flux ($Lm^{-2}h^{-1}$); Jw_1 is the last *PWP* measured before the fouling experiment ($Lm^{-2}h^{-1}$); Jw_2 is the last *PWP* of post fouling pure water experiment ($Lm^{-2}h^{-1}$); *Jp* is the last flux ($Lm^{-2}h^{-1}$) of the fouling test; *Compac*: fraction of reduction caused by compaction, i.e., flux reduction normalized by Jw_0; R_{total} is the total flux reduction due to fouling (i.e., both irreversible and reversible fouling) normalized by Jw_1; R_{irr} is the irreversible fouling flux reduction due to irreversible fouling normalized by Jw_1; R_{rev} is the reversible fouling flux reduction normalized by Jw_1.

The results are summarized in Table 2. From this table, it is evident that for the PES membrane the flux reduction, due to both by compaction and fouling, was not severe. Negative value of R_{rev} means *Jw2* was slightly lower than *Jp*. Flux reductions of EPES-250 were severer than PES both by compaction and fouling. The compaction is likely due to the softness of the nanofiber layer, as weak mechanical strength of electrospun nanofiber membranes is well documented [28]. Flux reduction in the ORW filtration is possibly due to severe concentration polarization caused by the stagnant ORW in the nanofiber layer. Some of the foulants filled up the spaces between nanofibers, causing severe irreversible fouling. Note that it is irreversible based on a tangential cleaning step, in which the flow is unlikely to penetrate the nanofiber layer and remove the accumulated foulants. It should be noted that R_{rev} is based on the flux achieved after the tangential wash, which is not as intensive a cleaning procedure as backwashing or chemical cleaning.

3.3. Filtration of protein solutions

The fouling test was conducted for 4 hr with BSA solution for all the series 4 PES and EPES membranes and the results are shown in Table 3. Compared with the *PWP* data shown in Table 1, the fluxes for the BSA feed solution are much lower. Moreover, the EPES membranes were fouled to a much greater extent than the PES membrane. Nevertheless, the fluxes of EPES membranes were higher than that of the PES membrane. Due to the high speed of fouling, one could hypothesize that fouling is caused by both concentration polarization and sorption of the proteins onto and into the electro-spun PVDF layer, which has hydrophobic characteristics. However, if the fouling is associated with the penetration of the foulant within the PVDF nanofiber layer, one would expect that the degree of flux reduction would be proportional to the PVDF nanofiber layer thickness. There was a slight trend of greater flux reduction for greater electrospinning time, however the BSA solution fluxes of all the electrospun membranes was higher than that of the PES membranes. In Table 3, the flux of the PES is lower than the EPESs membranes, without exception. The difference was very small between EPES- 250 and EPES- 125.

Table 4 shows the results of the filtration tests for different proteins using Series 4 PES and EPES-250 membranes. The table shows the fluxes of the EPES-250 membrane are higher than those for the PES membrane, for each of the protein solutions tested. As well, the flux decreases progressively from Trypsin to BSA, as the molecular weight of protein increases. This phenomenon is due to fouling by the solute protein, and the severer pore blocking by the larger proteins.

3.4. Scanning electron microscopic (SEM) image analysis

Figure 3 shows the SEM images of PES and PES-250 surfaces before and after filtration experiments with ORW. Figure 3a,c are the surface images of PES and EPES-250, respectively, before the ORW filtration test. Both surfaces look clean. PES membrane is relatively smooth, while EPES-250's surface is covered by electro-spun nanofibers with a small number of beads. By applying ImageJ analysis for the picture given in Figure 3c, the average pore size of the ENM was evaluated to be 0.75 µm. Figure 3b,d are surface images of the PES and EPES-250, respectively, after ORW filtration. Interestingly, on the surface of the PES there appears to be a wavy pattern, which could possibly be created by the stream lines of the feed ORW. The EPES-250 surface is uniformly covered by foulants without showing any patterns, and the foulant seems to partially fill the voids in between the nanofibers. A higher magnification (Figure 4) image of the surface was taken to provide a clearer image; this allowed the measurement of the sizes of the foulant spheres. As shown in the figure, the diameters of large spheres were slightly less than 1 µm.

Figure 5 shows the cross-sectional images of PES and EPES before and after the ORW filtration test. Figure 5a shows the asymmetric structure of PES with a skin layer at the top surface and Figure 5c shows the electro-spun nanofiber layer coated on top of PES. Figure 5b shows the cross-section of the PES membrane after ORW filtration, in which there is a foulant layer on top and the support layer with a finger-like structure on the bottom. Figure 5d shows a higher magnification image of the nanofiber part of the fouled EPES-250 membrane, which shows some foulant particles trapped between fibers of the electro-spun nanofiber layer.

Figure 6 shows a typical example for the thickness measurement of the electro-spun nanofiber layer within virgin membranes. Based on the images of 5 to 7 different spots, the thickness of the nanofiber layer ranged 8 to 16, 19 to 56 and 89 to 93 µm, respectively, for the EPES-25, -125 and -250 membranes.

Increasing layer thickness with electrospinning time is illustrated in Figure 7. This graph shows almost a linear trend of increase for EPES-25 to EPES-250. However, the thickness was not uniform and varied along the cross sections of membrane. The upper portion in each column indicates the range of thickness in each EPES membrane.

Table 2
Normalised flux decrease of Series 1 PES and EPES-250 by ORW due to compaction and fouling.

Parameter	PES	EPES-250
Compac	0	0.094
R_{total}	0.09	0.43
R_{irr}	0.11	0.32
R_{rev}	-0.02	0.12

Table 3
Permeate flux of series 4 membranes when the feed is BSA solution.

Membrane	PES	EPES- 250	EPES- 125	EPES- 25
Average Fouling Flux ($Lm^{-2}h^{-1}$)	84.3 ± 3.5[a]	91.5 ± 5.57	98.9 ± 4.4	102.2 ± 2.8

[a] Standard deviation

Table 4
Permeate Flux of Series 4 PES and EPES-250 for various feed protein solutions.

Protein	Trypsin (MW 2300)		Pepsin (MW 34500)		Egg albumin (MW 42700)		BSA (MW 67000)	
Membrane	PES	EPES-250	PES	EPES-250	PES	EPES-250	PES	EPES-250
Average ($Lm^{-2}h^{-1}$)	92.2 ± 1.7[a]	127.1 ± 14.8	82.4 ± 1.96	108.5 ± 3.96	78.4 ± 1.70	93.5 ± 4.08	84.3 ± 3.5	91.5 ± 5.57

[a] Standard deviation

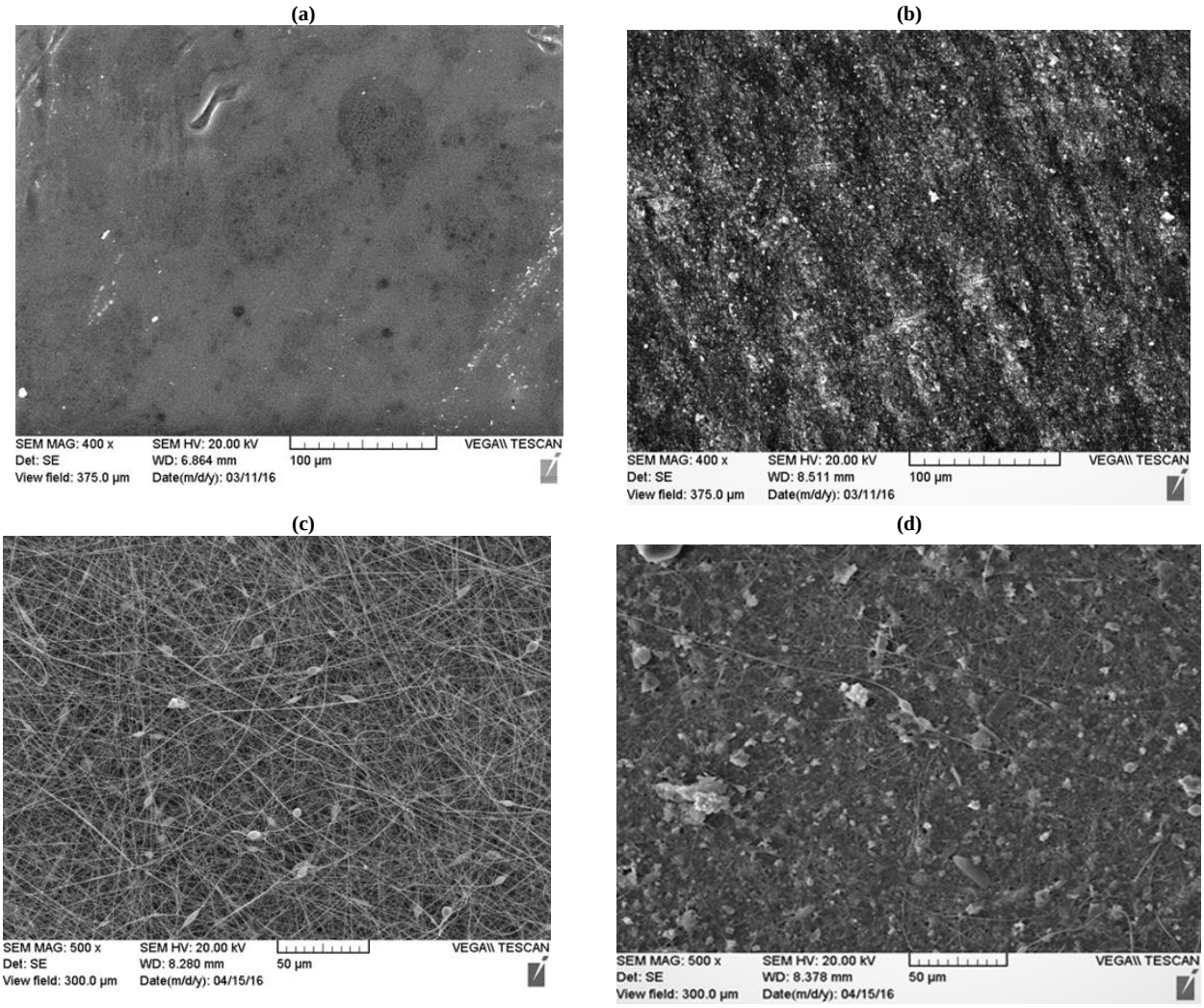

Fig. 3. SEM surface images of a) PES before b) PES after the filtration of ORW c) EPES-250 before and d) EPES-250 after filtration of ORW.

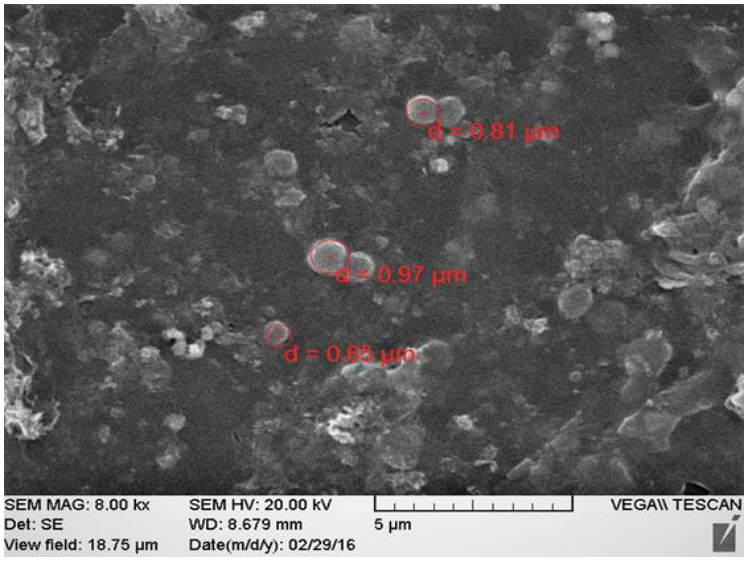

Fig. 4. SEM image (with 8K magnification) of the surface of the PES membrane with measurement of foulant particle sizes.

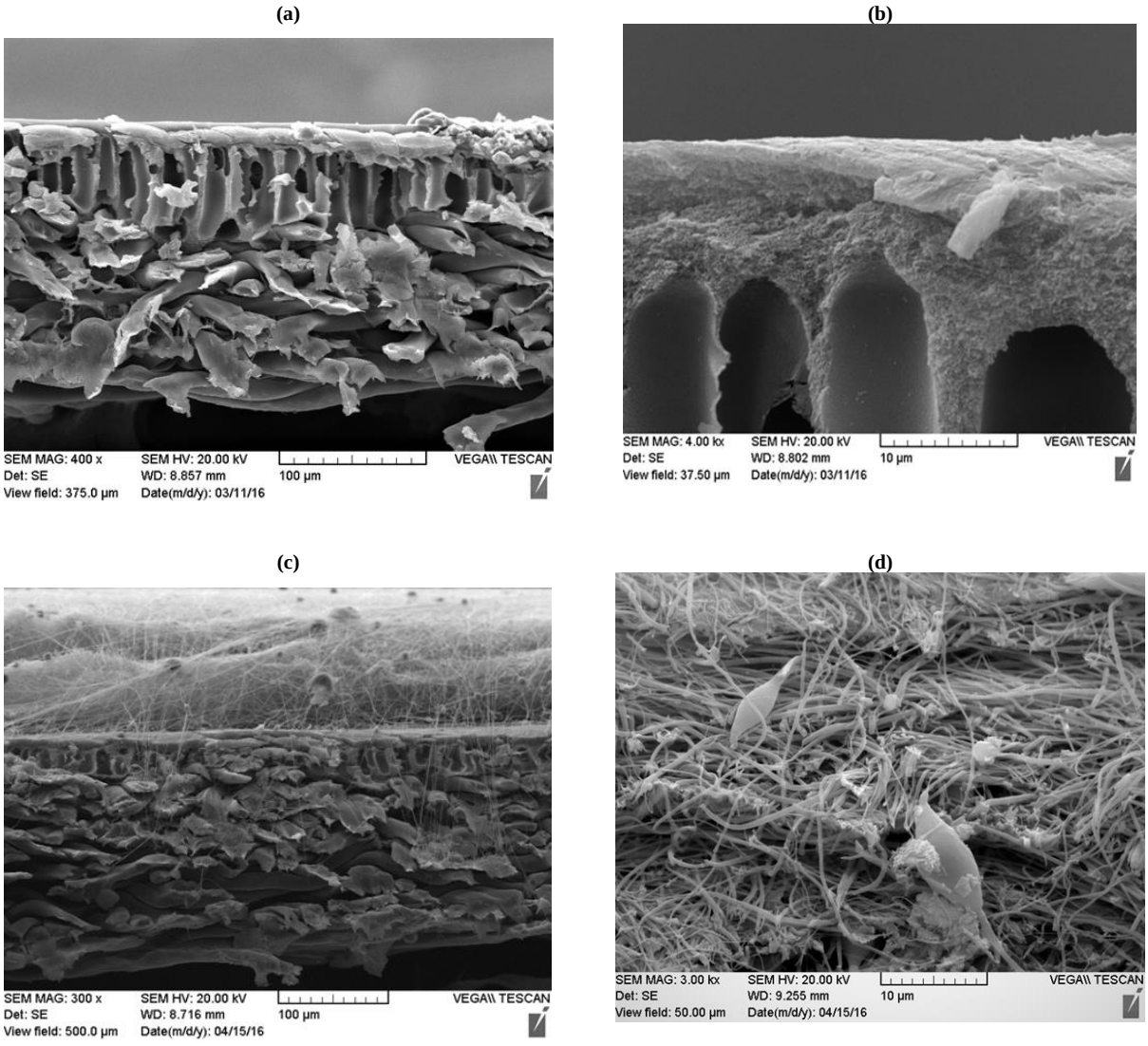

Fig. **5**. Cross-sectional images of a) PES membrane before filtration; b) PES membrane after filtration of ORW; c) EPES-250 membrane before filtration; and d) EPES-250 membrane after filtration of ORW.

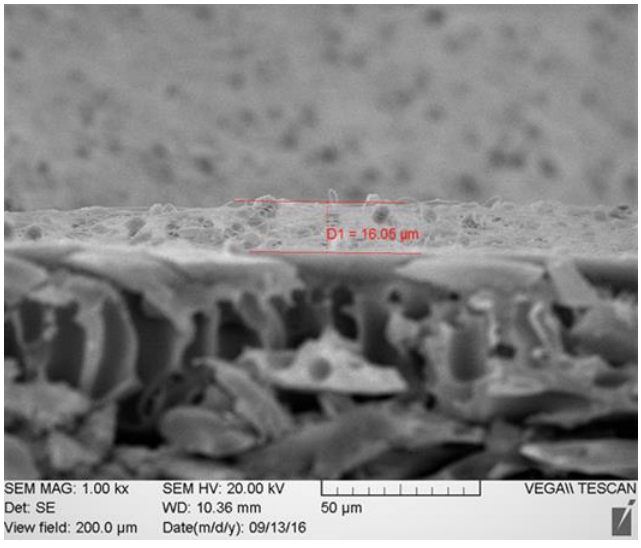

Fig. **6**. Cross-sectional images of the virgin EPS-25 membrane with 16 µm thick nanofiber layer.

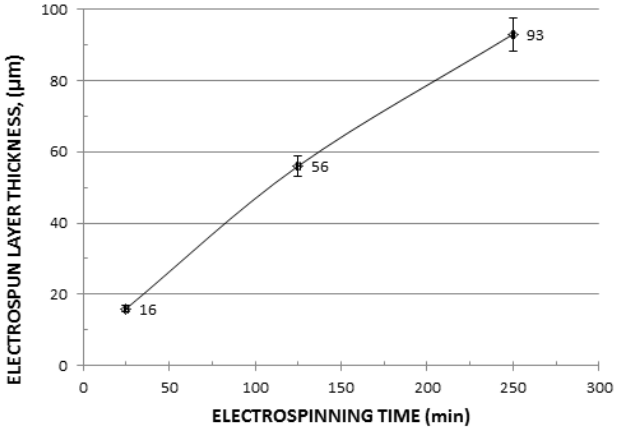

Fig. 7. Thickness of electrospun layer versus electrospinning time.

3.5. Contact angle measurements

Results of the contact angle measurement are summarized in Table 5. Table 5 shows that the contact angle increases progressively from PES to EPES-125 as the electro-spinning period increases and then levels off.

3.6. Pore size of the composite membrane

According to the method proposed by Kanagaraj et al. [27], the radius of the membrane pore is given by:

$$Pore\ radius = 100\times(r/R) \quad (7)$$

where r is the Stokes radius (nm) of the solute and R is the percentage of solute rejection. As seen in Table 6, using this simple equation and the trypsin, egg albumin and BSA removal data, the membrane's pore radii are estimated as 1.38, 3.34 and 3.59 nm, respectively. The pore size obtained by this method depends on the solute but they are in the range of ultrafiltration membranes and much less than the pore size of the ENM (0.75 µm).

As well, the molecular weight cut off reported by the manufacturer was 3 kD. The solute removals by the EPES-250 membrane and the PES membrane are very similar. Thus, it can be reasonably concluded that the solute rejection took place at the substrate PES membrane not at the nanofiber layer.

4. Conclusions

From the experimental results the following conclusions can be drawn. When the commercial PES membrane was coated with a PVDF electrospun nanofiber layer, the coated layer thickness was proportional to the electrospinning period. In pure water permeation (PWP) experiments, the PVDF nanofiber/PES composite membranes exhibited higher PWP fluxes than the substrate PES membrane, which confirms the results of Dobosz et al [16]. The reason for the flux enhancement is not yet fully understood. By the filtration study with Ottawa River Water (ORW), it was found that the composite membranes are more susceptible to compaction than the substrate PES membrane due to the weak mechanical strength of the nanofiber layer. As well, cleaning by tangential flow showed that the fouling of substrate PES membrane is reversible while the fouling of the composite membrane is irreversible. The foulants likely filled in the spaces between the nanofibers. From the filtration experiments with the solutions of different proteins, it was concluded that the separation took place not by the nanofiber layer but by the substrate membrane.

Table 5
Summary of contact angle measurements.

PES	EPES-25	EPES- 125	EPES- 250
62.7 ± 0.57[a]	85.0 ± 0.74	109.2 ± 1.34	109.9 ± 1.09

[a] Standard deviation

Table 6
Molecular weight, diffusivity and radius of protein.

Protein	Trypsin	Pepsin	Egg Albumin	BSA
M (Dalton)	2300	34500	42700	67000
D (m^2s^{-1}) x 10^{10}	2.122	0.8614	0.8023	0.6905
r (nm)	1.156	2.848	3.057	3.552
R (%) by EPES-250	82	-	92	99
R (%) by PES	85		98	96

Acknowledgements

This research was supported by Natural Sciences and Engineering Research Council of Canada.

References

[1] https://www.donaldson.com/content/dam/donaldson/engine-hydraulics-bulk/literature/north-america/air/F111274-ENG/Ultra-Web-Air-Filtration-Nanofiber-Technology.pdf

[2] http://electrospintech.com/products.html#.W7ThXGzQbIU

[3] Q. Liu, Z. Chen, X. Pei, C. Guo, K. Teng, Y. Hu, Z. Xu, X. Qian, Review: applications, effects and the prospects for electrospun nanofibrous mats in membrane separation, J. Mater. Sci. 55 (2020) 893-924. DOi: 10.1007/s10853-019-040

[4] Z. Xu, X. Li, K. Teng, B. Zhou, M. Ma, M. Shan, K. Jiao, X. Qian, J. Fan, High flux and rejection of hierarchical composite membranes based on carbon nanotube network and ultrathin electrospun nanofibrous layer for dye removal, J. Membr. Sci. 535 (2017) 94-102. DOi: 10.1016/j.memsci.2017.04.029

[5] X. Li, K. Teng, J. Shi, W. Wang, Z. Xu, H. Deng, H. Lv, F. Li, Electrospun preparation of polylactic acid nanoporous fiber membranes via thermal-nonsolvent induced phase separation, J. Taiwan Inst. Chem. Eng. 60 (2016) 636-642. 10.DOi: 10. 1016/j.jtice.2015.11.012

[6] J. Shi, T. Wu, K.Teng, W. Wang, M. Shan, Z. Xu, H. Lv, H. Deng, Simultaneous electrospinning and spraying toward branch-like nanofibrous membranes functionalised with carboxylated MWCNTs for dye removal, Mater. Lett. 166 (2016), 26-2. DOi: 10.1016/j.matlet.2015.12.024

[7] J.W.Wu, J. Zhang, Y.L. Kang, G. Wu, S.C. Chen, Y.Z. Wang, Reusable and recyclable superhydrophilic electrospun nanofibrous membranes with in situ Co-cross-linked polymer–chitin nanowhisker network for robust oil-in-water emulsion separation, ACS. Sustainable Chem. Eng. 6 (2018) 1753–1762. https://pubs.acs.org/doi/abs/10.1021/acssuschemeng.7b03102

[8] K. Yoon, B.S. Hsiao, B. Chu, Formation of functional polyethersulfone electrospun membrane for water purification by mixed solvent and oxidation processes, Polymer 50 (2009) 2893-2899. https://doi.org/10.1016/j.polymer.2009.04.047

[9] M.S. Islam, M.S. Rahaman, J.R. McCutcheon, High flux polyvinyl acetate-coated electrospun Nylon 6/SiO_2 composite microfiltration membrane for the separation of oil-in-water emulsion with improved antifouling performance, J. Membr. Sci. 537 (2017) 297-309. https://doi.org/10.1016/j.memsci.2017.05.019

[10] R. Gopal, S. Kaur, Z. Ma, C. Chan, S. Ramakrishna, T. Matsuura, Electrospun nanofibrous filtration membrane, J. Memr. Sci. 281 (2006) 581-586. https://doi.org/10.1016/j.memsci.2006.04.026

[11] T.M. Yeh, L. Yang, X. Wang, D. Mahajan, B.S. Hsiao, B. Chu, Polymeric nanofibrous composite membranes for energy efficient ethanol dehydration, J. Renew. Sustain. Ener. 4 (2012) 04140. https://doi.org/10.1063/1.4739760

[12] C. Feng, K.C. Khulbe, T. Matsuura, R. Gopal, S. Kaur, S. Ramakrishna, M. Khayet, Production of drinking water from saline water by air-gap membrane distillation using polyvinylidene fluoride nanofiber membrane, J. Membr. Sci. 311 (2008) 1–6. https://doi.org/10.1016/j.memsci.2007.12.026

[13] Q. Yang, J. Lei, D.D. Sun, D. Chen, Forward osmosis membranes for water reclamation, Sep. Purif. Rev. 45 (2016) 93-107. https://doi.org/10.1080/15422119.2014.973506

[14] N. Chitpong, S.M. Husson, Nanofiber ion-exchange membranes for the rapid uptake and recovery of heavy metals from water, Membranes 6 (2016), 59-74. https://doi.org/10.3390/membranes6040059

[15] K. Yoon, K. Kim, X. Wang, D. Fang, B.S. Hsiao, B. Chu, High flux ultrafiltration membranes based on electrospun nanofibrous PAN scaffolds and chitosan coating, Polymer 47 (2006) 2434-2441. https://doi.org/10.1016/j.polymer.2006.01.042

[16] K.M. Dobosz, C.A. Kuo-Leblanc, T.J. Martin, J.D. Schiffman, Ultrafiltration membranes enhanced with electrospun nanofibers exhibit improved flux and fouling resistance, Ind. Eng. Chem. Res. 56 (2017) 5724–5733. https://doi.org/10.1021/acs.iecr.7b00631

[17] S. Ma, L. Song, Numerical study on permeate flux enhancement by spacers in a crossflow reverse osmosis channel, J. Membr. Sci. 284 (2006) 102−109. https://doi.org/10.1016/j.memsci.2006.07.022

[18] Y.-J. Won, S.-Y. Jung, J.-H. Jang, J.-W. Lee, H.-R. Chae, D.-C. Choi, A.-K. Hyun, C.-H. Lee, P.-K. Park, Correlation of membrane fouling with topography of patterned membranes for water treatment, J. Membr. Sci. 498 (2016) 14−19. https://doi.org/10.1016/j.memsci.2015.09.058

[19] H. Wang, J. Ding, L. Dai, X. Wang, T. Lin, Directional water-transfer through fabrics induced by asymmetric wettability, J. Mater. Chem. 20 (2010), 7938-7940. https://doi.org/10.1039/C0JM02364G

[20] H.T. Dang, R.M. Narbaitz, T. Matsuura, K.C. Khulbe, Comparison of commercial and experimental ultrafiltration membranes via surface property analysis and fouling tests, Water Qual. Res. J. 41 (2006) 84-93. https://doi.org/10.2166/wqrj.2006.009

[21] L. Zoka, Effect of surface coating with electrospun nanofibers on the performance of the ultrafiltration membrane. MASc thesis, Dept. of Civil Engineering, University of Ottawa, Ottawa, Canada, 2018.

[22] B. Xu, R.M. Narbaitz, Improved membrane pretreatment of high hydrophobic natural organic matter (NOM) waters by floatation, J. Membr. Sci. 518 (2016) 120–130. https://doi.org/10.1016/j.memsci.2016.02.056

[23] N. Pezeshk, D. Rana, R.M. Narbaitz, T. Matsuura, Novel modified PVDF ultrafiltration flat-sheet membranes, J. Membr. Sci. 389 (2012) 280-286.

https://doi.org/10.1016/j.memsci.2011.10.039

[24] J. Efome, D. Rana, T. Matsuura, C. Lan, Enhanced performance of PVDF nanocomposite membrane by nanofiber coating: A membrane for sustainable desalination through MD, Water Res. 89 (2016) 39-49. https://doi.org 10.1016/j.watres.2015.11.040

[25] N. Pezeshk, Modified PVDF ultrafiltration flat sheet membranes for water treatment. MASc thesis, Dept. of Civil Engineering, University of Ottawa, Ottawa, Canada, 2010.

[26] D.B. Mosqueda-Jimenez, R.M. Narbaitz, T. Matsuura, Membrane fouling test: Apparatus evaluation, J. Environ. Eng.-ASCE, 30 (2004) 90-99. https://doi.org/10.1061/(ASCE)0733-9372(2004)130:1(90)

[27] P. Kanagaraj, S. Neelakandan, A. Nagendran, Poly(ether imide) membranes modified with charged surface-modifying macromolecule - Its performance characteristics as ultrafiltration membranes, J. Appl. Polym. Sci. 131(2014) 1-8. https://doi.org/10.1002/app.40320

[28] L. Huang, S.S. Manickam, J.R. McCutcheon, Increasing strength of electrospun nanofiber membranes for water filtration using solvent vapor, J. Membr. Sci. 436 (2013) 213-220. https://doi.org/10.1016/j.memsci.2012.12.037